CONF-970158--1

ANL/PHY/CP--92134

Precise Measurement of the Neutron Magnetic Form Factor from Quasielastic $^3\vec{H}e(\vec{e},e')$

H. Gao*

Argonne National Laboratory, Argonne, IL 60439-4843, U.S.A.

Abstract

Polarized ^{3}He targets have proven to be a useful tool for studying the electric and magnetic form factors of the neutron, and the spin structure of the neutron. The neutron magnetic form factor at low Q^2 was determined previously at MIT-Bates from the quasielastic $^3\vec{H}e(\vec{e},e')$ process. New experiment was planned at TJNAF to systematically measure the inclusive ^{3}He quasielastic transverse asymmetry, $A_{T'}$, at Q^2 = 0.1 - 0.5 (GeV/c)^2 with high statistical and systematic accuracy. A 2% statistical uncertainty is aimed at all the proposed values of Q^2, and 3% systematic uncertainty for $A_{T'}$ can be achieved for this experiment. The precise data will constrain theoretical calculations of ^{3}He quasielastic asymmetry. Furthermore, the neutron magnetic form factor at Q^2 = 0.1 - 0.5 (GeV/c)^2 will be extracted from the measured asymmetries with an overall uncertainty of 2%. Precise measurements of G_M^n at low Q^2 will resolve the discrepancy among the existing data in the same Q^2 region.

I. INTRODUCTION

Electromagnetic form factors are of fundamental importance for an understanding of the underlying structure of nucleons. Knowledge of the distribution of charge and magnetization

---

*Corresponding author. Tel. +1 630 252 7267, fax +1 630 252 3903, e-mail gao@anl.gov

within the nucleons provides a sensitive test of models based on QCD, as well as a basis for calculations of processes involving the electromagnetic interaction with complex nuclei. Due to the lack of a free neutron target, the neutron electromagnetic form factors are known with less precision than the proton electric and magnetic form factors. They have been deduced in the past from elastic or quasielastic electron-deuteron scattering. This procedure involves considerable model dependence.

Recently, there have been great interests in measuring the neutron magnetic form factor, G_M^n at low Q^2 using deuteron targets [1-3], motivated largely by the poor quality of the previous data on G_M^n at low Q^2 and also by the growing interests in measuring the neutron electric form factor, G_E^n at low Q^2. Precise measurements of the neutron magnetic form factor at low Q^2 is also very important in terms of determining the strange magnetic and electric form factor of the nucleon, $G_M^{(s)}$ and $G_E^{(s)}$ from parity-violation experiments. For e-p elastic scattering at backward-angle, up to radiative corrections G_M^n and $G_M^{(s)}$ enter the parity-violating asymmetry with equal weights [4]. Thus, an accurate extraction of $G_M^{(s)}$ requires very accurate knowledge of G_M^n. Likewise as far as a determination of $G_E^{(s)}$ is concerned for e-p elastic scattering at forward angle, the error in G_M^n is roughly three times more important than the uncertainty in G_E^n because of the premultiplying factor of the proton magnetic moment, μ_p in the parity-violating asymmetry [4].

The development of polarized targets and beams has allowed more complete studies of electromagnetic structure than has been possible with unpolarized reactions. In quasielastic scattering, the spin degrees of freedom introduce new response functions into the inclusive cross section, thus providing additional information on nuclear structure [5]. ^{3}He is an interesting nucleus for polarization studies because its ground state wave function is predominantly a spatially symmetric S state in which the spin of the nucleus is carried mainly by the unpaired neutron. Therefore, inelastic scattering of polarized electrons from polarized ^{3}He in the vicinity of the quasielastic peak should be useful for studying the neutron electromagnetic form factors. This idea was first investigated by Blankleider and Woloshyn in closure approximation [6]. Friar *et al.* [7] have studied the model dependence in the spin structure of the ^{3}He wave function and its effect on the quasielastic asymmetry. The plane wave impulse approximation (PWIA) calculations performed independently by two groups [8,9] using a spin-dependent spectral function show that the spin-dependent asymmetry is very sensitive to the neutron electric or magnetic form factors at certain kinematics near the top of the quasielastic peak. Following experiments [10,11], the neutron magnetic form factor at low Q^2 was extracted for the first time [12] from the measured quasielastic transverse asymmetry, $A_{T'}$ from $^3\vec{H}e(\vec{e},e')$. The measurement was limited by the statistical uncertainty because a relatively low-density polarized ^{3}He target was employed. Recently, Ishikawa *et al.* [13] performed new calculation of the ^{3}He inclusive spin-dependent quasielastic asymmetries in which final state interactions (FSI) were included. Calculations which include FSI and meson-exchange currents (MEC) are currently underway [14]. With the new calculations and the development of a high pressure spin-exchange polarized ^{3}He target, a new experiment [15] was planned at the Thomas Jefferson National Accelerator Facility (TJNAF, formly CEBAF) to precisely determine G_M^n at low Q^2.

II. ^{3}HE SPIN-DEPENDENT ASYMMETRY

The spin-dependent asymmetry for longitudinally polarized electrons scattered from a polarized spin-$\frac{1}{2}$ nuclear target can be written [5] as

$$A = -\frac{\cos\theta^* v_{T'} R_{T'} + 2\sin\theta^* \cos\phi^* v_{TL'} R_{TL'}}{v_L R_L + v_T R_T}, \tag{1}$$

where the v_K are kinematic factors, and θ^* and ϕ^* are the polar and azimuthal angles of the target spin with respect to the 3-momentum transfer vector $\mathbf{q}$. $R_L(Q^2,\omega)$ and $R_T(Q^2,\omega)$ are the longitudinal and transverse nuclear response functions associated with the unpolarized cross section and are functions of the square of the 4-momentum transfer Q^2 and the electron energy loss ω. $R_{T'}(Q^2,\omega)$ and $R_{TL'}(Q^2,\omega)$ are the two response functions arising from the polarization degrees of freedom. $R_{T'}$ is a transverse response function and $R_{TL'}$ represents the interference between the transverse and the longitudinal multipoles. By orienting the target spin at $\theta^* = 0^\circ$ or $\theta^* = 90^\circ$, corresponding to the spin direction either along the 3-momentum transfer vector $\mathbf{q}$ or normal to it, one can select the transverse asymmetry $A_{T'}$ (proportional to $R_{T'}$) or the transverse-longitudinal asymmetry $A_{TL'}$ (proportional to $R_{TL'}$). PWIA calculations [5-9] neglecting FSI and MEC, as well as the recent calculation by Ishikawa *et al.* [13] including FSI, indicate that the transverse asymmetry $A_{T'}$ is very sensitive to the square of the neutron magnetic form factor, ${G_M^n}^2$.

For longitudinally polarized electrons scattering elastically from a polarized ^{3}He nuclear target, the elastic asymmetry can be expressed in terms of the ^{3}He charge and magnetic form factors, F_c and F_m, as

$$A_{el} = \frac{\Delta}{\Sigma} = -\frac{2\tau\mu_A^2 v_{T'}\cos\theta^* F_m^2 + 2\sqrt{2\tau(1+\tau)}\mu_A Z v_{TL'}\sin\theta^*\cos\phi^* F_m F_c}{(1+\tau)Z^2 v_L F_c^2 + 2\tau\mu_A^2 v_T F_m^2} \tag{2}$$

where the form factors have been normalized to

$$F_c(Q^2 = 0) = F_m(Q^2 = 0) = 1. \tag{3}$$

In this formula Z is the nuclear charge, μ_A is defined in terms of the magnetic moment of ^{3}He as $(m_{\mathrm{He}}/m_n)\mu_{\mathrm{He}}$, and all other variables are kinematic factors defined in Ref. [5]. The experimental elastic asymmetry is diluted by the product of the beam and target polarizations. Thus, the product of the beam and target polarization can be determined by measuring the elastic asymmetry using the known ^{3}He elastic form factors.

III. EXPERIMENTS

A. MIT-Bates Experiment 88-25

The experiment [12] was performed at the MIT-Bates Linear Accelerator Center using a 370 MeV longitudinally polarized electron beam. The source of the polarized electrons was a crystal of GaAs optically pumped by a Ti:sapphire laser driven with an Ar-ion laser. A Wien spin rotator was employed to produce longitudinally polarized electrons at the target. The average beam current during the experiment was 25 μA and the average beam polarization was determined using a Møller apparatus [16] to be 36.5%.

The polarized ^{3}He target used in this experiment was a double-cell system consisting of a glass pumping cell and a copper target cell. The target was polarized by the metastability-exchange optical pumping technique [17]. A weak electric discharge was maintained in the pumping cell to excite ^{3}He atoms into the metastable state. The optical pumping light was supplied by a Nd-doped lanthanum magnesium hexaluminate crystal (LNA) pumped by a krypton arc lamp in a Laser Application 9560 cavity. The target was operated at 13 K during the experiment with a ^{3}He gas pressure of 2.2 torr. The target wall was coated with a thin layer of nitrogen to maintain a sufficiently long relaxation time at low temperature. A holding field of 36 gauss provided by a pair of Helmholtz coils defined the target spin quantization axis. The target spin direction was aligned at an angle of 42.5° to the electron beam. High voltage on a Pockels cell was varied to change the helicity of the circularly polarized laser light, thus reversing the target spin direction. The target spin was flipped several times a day to minimize systematic uncertainties. The pumping cell polarization was measured continuously by monitoring the circular polarization of the 668-nm line excited by the ^{3}He discharge. The target polarization was inferred from the polarization of the pumping cell and the time constants of the coupled system. This optical measurement of the ^{3}He nuclear polarization was calibrated by an NMR measurement [18] with an accuracy of 2%. With $25\mu A$ of beam, the target polarization was 38% or greater. With no depolarization from the beam, the target polarization was typically higher by a factor of 1.15.

The scattered electrons were detected in the Medium Energy Pion Spectrometer (MEPS) configured at an electron scattering angle $\theta = 91.4^\circ$ to the left of the beam. The spectrometer central momentum was 250 MeV/c corresponding to $Q^2 = 0.19$ (GeV/c)^2 and $\theta^* = 8.9^\circ$ or 171.1° for positive or negative target polarization, respectively. The MEPS spectrometer had a momentum acceptance of ±10% and an extended target acceptance of 2 cm resulting in a target thickness of 3.3×10^{18} cm^{-2}.

The transverse asymmetry $A_{T'}$ was extracted from the spin-dependent quasielastic inclusive cross section as a function of the electron energy loss ω for a total beam charge of 6529 μA-h. Corrections have been made for the empty target background, the elastic radiative tail and the quasielastic radiative effect. The measured quasielastic transverse asymmetry $A_{T'}(\omega)$ is shown in Fig. 1 along with various calculations at the kinematics of the MIT-Bates experiment 88-25 [12].

To determine ${G_M^n}^2$ from the measured asymmetry $A_{T'}$, the calculation of Ishikawa *et al.* [13] was employed. The standard dipole form factor parametrization [21] gives

$$\frac{G_M^n}{\mu_n} = \frac{G_M^p}{\mu_p} = G_E^p = G_D = \left[1 + \frac{Q^2}{0.71}\right]^{-2}, \tag{4}$$

where Q^2 is in (GeV/c)^2. Fig. 2 shows G_M^n extracted from the Bates experiment [12], together with the world data in the low Q^2 region. The error of the MIT-Bates [12] measurement is dominated by the statistical uncertainty.

B. TJNAF Experiment E95-001

The TJNAF experiment [15] will employ a longitudinally polarized electron beam, a spin-exchange polarized ^{3}He target, and the Hall A High Resolution Spectrometers (HRS). Quasielastic kinematics are chosen for the inclusive $^3\vec{H}e(\vec{e},e')$ reaction. The single-arm measurement of the spin-dependent quasielastic transverse asymmetry will be performed by using the Hall A electron-arm HRS spectrometer for detecting the quasielastically scattered electrons. The Hall A hadron-arm HRS spectrometer will be dedicated to measure the ^{3}He elastic asymmetry to serve as a beam and target polarization monitor. Single-arm measurements from $^3\vec{H}e(\vec{e},e')$ reaction were proposed at the quasielastic kinematics with an incident electron beam energies of 0.8 and 1.6 GeV, and at electron scattering angles of 20.8°, 23.6°, 24.5°, 28.01°, and 34.9°, covering a Q^2 region from 0.1 to 0.5 (GeV/c)^2, in steps of 0.1 (GeV/c)^2. The target spin direction will be aligned along the three-momentum transfer vector, **q** and the ^{3}He spin-dependent quasielastic transverse asymmetry, $A_{T'}(\omega)$ will be formed by varying the helicity of the polarized electron beam. The principle of the polarized electron beam at TJNAF is similar to that of the MIT-Bates Laboratory as described earlier. Given the technical developments currently achieved with strained GaAs cathodes at SLAC (E143, E154) and other places, high electron polarization (80%) is possible to achieve at TJNAF.

The polarized ^{3}He target will be based on the principle of spin exchange between optically pumped alkali-metal vapor and noble-gas nuclei [29-31]. The design will be similar in many ways to that used in E-142, an experiment at SLAC to measure the spin dependent structure function of the neutron [32]. A central feature of the target will be sealed glass target cells, which will contain a ^{3}He pressure of about 12-13 atmospheres. The cells will have two chambers, an upper chamber in which the spin exchange takes place, and a lower chamber, through which the electron beam will pass. In order to maintain the appropriate number density of alkali-metal (which will probably be Rb) the upper chamber will be kept at a temperature of 170–200°C using an oven constructed of the high temperature plastic Torlon. With a density of 2.5×10^{20} atoms/cm^3, and a lower cell length of 40 cm, the target thickness will be 1.0×10^{22} atoms/cm^2. For an incident electron beam current of 10 to 15 μA, a target polarization of $40 - 45\%$ is expected. To polarize such a high density ^{3}He target, approximately 20–24 Watts of "usable" light at 795 nm will be required. "Usable" light means the part of the light that can be readily absorbed by the Rb. The absorption line of the Rb will have a full width of several hundred GHz at the high pressures of ^{3}He at which the target will be operated. New emerging diode laser technology is advantageous to economically pump the target. While some studies of the use of diode lasers for spin-exchange optical pumping do exist in the literature [33], actual demonstrations of high polarizations in cells suitable for targets are much more recent [34]. For the recently finished SLAC experiment E154, the diode laser system was used for the spin exchange polarized ^{3}He target. Large Helmholtz coils will be used to apply a static magnetic field of about 20 Gauss to define the spin quantization axis. Details of the target is given in Ref. [35].

The uncertainty from model dependence in extracting the neutron magnetic form factor was studied carefully [12] following the approach by Friar *et al.* [7], and the uncertainty was determined to be 3% in ${G_M^n}^2$. In Ref. [12] the measured quasielastic asymmetry, $A_{T'}(\omega)$, averaged over the experimental ω acceptance was used to extract ${G_M^n}^2$ because of the limitation of the statistics of the measurement. The planned TJNAF experiment [15] will achieve 2% statistical and 3% systematic uncertainties for $A_{T'}$ measurements on top of the ^{3}He quasielastic peak (20 MeV bin for the electron energy transfer) at all proposed values of Q^2. Therefore, the uncertainty from model dependence can be further reduced by using the precisely measured proton form factors at the corresponding Q^2 of the proposed measurement for calculating $A_{T'}$ on top of the ^{3}He quasielastic peak. Though G_E^n is known rather poorly in the Q^2 region of this experiment, its contribution to $A_{T'}$ is negligible. The model-dependent uncertainty in extracting G_M^n using the calculations of Ishikawa [13] *et al.* is estimated to be 1.0% based on the results for different N-N potentials. To emphasize for TJNAF experiment E95-001 [15], only $A_{T'}$ in close vicinity of the quasielastic peak ($\omega_0 - 10$ MeV $\leq \omega \leq \omega_0 + 10$ MeV) will be used in extracting G_M^n, a procedure expected to be much less sensitive to final state interactions, meson exchange currents, and relativistic effects. Currently, calculation of the ^{3}He inclusive spin-dependent quasielastic asymmetry which includes the final state interactions, meson exchange currents, and relativistic effects is underway [14]. Therefore, precise measurement of the ^{3}He $A_{T'}(\omega)$ is necessary to constrain theoretical calculations of $A_{T'}(\omega)$ to allow extracting G_M^n with high precision on top of the ^{3}He quasielastic peak.

By using a high density polarized ^{3}He target, one can achieve high statistical measurements at TJNAF. TJNAF Experiment E95-001 [15] was proposed to achieve a 2% statistical accuracy for $A_{T'}$ on top of the quasielastic peak at all proposed values of Q^2. In order not to limit the data by the systematic uncertainties associated with the determinations of the beam and target polarizations, the hadron HRS spectrometer will be employed as a monitor of the beam and target polarizations by simultaneously measuring the ^{3}He elastic asymmetry. The ^{3}He elastic charge and magnetic form factors at $Q^2 = 0.1, 0.2$ (GeV/c)^2 were determined by Rosenbluth separation [36] to overall uncertainties of 1.5%. Thus, by precisely measuring the elastic asymmetry at $Q^2 = 0.1, 0.2$ (GeV/c)^2, the product of the beam and target polarizations can be determined to an overall uncertainty of 3%. Fig. 3 shows the proposed measurements of $A_{T'}(\omega)$ with the anticipated statistical errors, together with the calculation by Ishikawa *et al.* [13] at proposed values of Q^2. Fig. 4 shows the recent data on G_M^n at low Q^2 together with the anticipated results on G_M^n from Experiment E95-001 [15], with the total errors being the quadratic sum of the statistical, systematic, and model-dependent uncertainties.

The author thanks Dr. S. Ishikawa for calculating the ^{3}He inclusive spin-dependent quasielastic transverse asymmetry, $A_{T'}(\omega)$, at the kinematics of the TJNAF experiment E95-001. This work is supported by the U.S. Department of Energy, Nuclear Physics Division, under contract No. W-31-109-ENG-38.

FIGURES

FIG. 1. The transverse asymmetry $A_{T'}$ as a function of electron energy loss ω. The solid circles are the data points from Ref. [12] with statistical uncertainties only. The dotted line is the calculation by Salmè *et al.* [19], the dash-dotted line is the calculation by Schulze *et al.* [20], and the solid line is the calculation by Ishikawa *et al.* [13].

FIG. 2. The square of the neutron magnetic form factor ${G_M^n}^2$, in units of the standard dipole parametrization, $(\mu_n G_D)^2$, in the low Q^2 region. The open squares are from Hughes *et al.* [22], the open diamonds are from the analysis by Kramer *et al.* [23] of the data from Grossetête *et al.* [24], the asterisks are from Braess *et al.* [23], the crosses are from Hanson *et al.* [25], the open circles are from Budnitz *et al.* [26], the open star is from Bartel *et al.* [27], the open triangle is from Stein *et al.* [28], and the solid diamonds are from Markowitz *et al.* [1] with the inner (outer) error bars being the statistical (total) uncertainties. The solid triangle shows the result from Anklin *et al.* [2] with the total error being the quadratic sum of the statistical and systematic errors, the solid stars are from Bruins *et al.* [3] with error bars being the quadratic sum of the statistical and systematic uncertainties. The solid circle is from Gao *et al.* [12] shown with the total uncertainty dominated by the statistical error. The data of Markowitz *et al.*, Hughes *et al.*, and Stein *et al.* have been displaced slightly to improve readability.

FIG. 3. Proposed measurements of $A_{T'}$ with errors being the statistical uncertainties at proposed values of Q^2, together with the calculations by Ishikawa *et al.* [13].

FIG. 4. The square of the neutron magnetic form factor ${G_M^n}^2$, in units of the standard dipole parametrization, $(\mu_n G_D)^2$, in the low Q^2 region. The anticipated $(G_M^n)^2$ values from experiment E95-001 are shown as solid squares with the total errors being the quadratic sum of the statistical, systematic, and model-dependent uncertainties.

REFERENCES

[1] P. Markowitz *et al.*, Phys. Rev. **C48**, R5 (1993).

[2] H. Anklin *et al.*, Phys. Lett. **B336**, 313 (1994).

[3] E.E.W Bruins *et al.*, Phys. Rev. Lett. **75**, 21 (1995).

[4] M.J. Musolf, T.W. Donnelly, J. Dubach, S.J. Pollock, S. Kowalski, and E.J. Beise, Phys. Report 239 (1,2), 1994.

[5] T.W. Donnelly and A.S. Raskin, Ann. Phys. **169**, 247 (Academic Press, New York, 1986).

[6] B. Blankleider and R.M. Woloshyn, Phys. Rev. **C29**, 538 (1984).

[7] J.L. Friar, B.F. Gibson, G.L. Payne, A.M. Bernstein, and T.E. Chupp, Phys. Rev. **C42**, 2310 (1990).

[8] C. Ciofi degli Atti, E. Pace, and G. Salmè, Phys. Rev. **C46**, R1591 (1992).

[9] R.-W. Schulze and P.U. Sauer, Phys. Rev. **C48**, 38 (1993).

[10] C.E. Woodward *et al.*, Phys. Rev. Lett. **65**, 698 (1990).

[11] A. K. Thompson *et al.*, Phys. Rev. Lett. **68**, 2901 (1992).

[12] H. Gao *et al.*, Phys. Rev. **C50**, R546 (1994); H. Gao, Ph.D. thesis, California Institute of Technology (unpublished, 1994).

[13] S. ishikawa, private communication.

[14] J. Golak, private communication.

[15] CEBAF proposal E95-001, Spokesperson: H. gao.

[16] J. Arrington, E.J. Beise, B.W. Filippone, T.G. O'Neill, W.R. Dodge, G.W. Dodson, K.A. Dow, and J.D. Zumbro, Nuclear Instrument and Methods **A311**, 39 (1992).

[17] R.G. Milner, R.D. McKeown, and C.E. Woodward, Nucl. Instrum. Methods Phys. Res., Sec. **A274**, 56 (1989); C.E. Jones *et al.*, Phys. Rev. **C47**, 110 (1993).

[18] W. Lorenzon, T.R. Gentile, H. Gao, and R.D. McKeown, Phys. Rev. **A47**, 468 (1993).

[19] C. Ciofi degli Atti, E. Pace and G. Salmè, in *Proceedings of the 6th Workshop on Perspectives in Nuclear Physics at Intermediate Energies*, ICTP, Trieste May 1993, (World Scientific); G. Salmè, private communication.

[20] R.-W. Schulze, private communication.

[21] S. Galster, H. Klein, J. Moritz, K.H. Schmidt, D. Wegener, and J. Bleckwenn, Nucl. Phys. **B32**, 221 (1971).

[22] E.B. Hughes, T.A. Griffy, M.R. Yearian, and R. Hofstadter, Phys. Rev. **139**, B458 (1965); *ibid.* **146**, 973 (1966).

[23] D. Braess and G. Kramer, Z. Phys. **189**, 242 (1966); D. Braess, D. Hasselman n and G. Kramer, Z. Phys. **198**, 527 (1967); D. Hasselmann and G. Kramer, DE SY 67/21 (September 1967).

[24] B. Grossetête, S. Jullian, and P. Lehmann, Phys. Rev. **141**, 1435 (1966).

[25] K.M. Hanson, J.R. Dunning, Jr., M. Goitein, T. Kirk, L.E. Price, and Richard Wilson, Phys. Rev. **D8**, 753 (1973).

[26] R.J. Budnitz *et al.*, Phys. Rev. **173**, 1357 (1968).

[27] W. Bartel *et al.*, Phys. Lett. **30B**, 285 (1969); *ibid.* **39B**, 407 (1972); Nucl. Phys. **B58**, 429 (1973).

[28] P. Stein, M. Binkley, R. McAllister, A. Suri, and W. Woodward, Phys. Rev. Lett. **16**, 592 (1966).

[29] M.A. Bouchiat, T.R. Carver and C.M. Varnum, Phys. Rev. Lett. **5**, 373 (1960).

[30] N.D. Bhaskar, W. Happer, and T. McClelland, Phys. Rev. Lett. **49**, 25 (1982).

[31] W. Happer, E. Miron, S. Schaefer, D. Schreiber, W.A. van Wijngaarden, and X. Zeng, Phys. Rev. A **29**, 3092 (1984).

[32] P.L. Anthony *et al.*, Phys. Rev. Lett. **71**, 959 (1993).

[33] M.E. Wagshul and T.E. Chupp, Phys. Rev. **A40**, 4447 (1989).

[34] W.J. Cummings *et al.*, Phys. ReV. **A51**, 4842 (1995).

[35] TJNAF proposal E94-010, Spokespersons: G. Cates, Z.-E. Meziani.

[36] A. Amroun *et al.*, Phys. Rev. Lett. **69**, 253 (1992); A. Amroun *et al.*, Nucl. Phys. **A579**, 596 (1994).

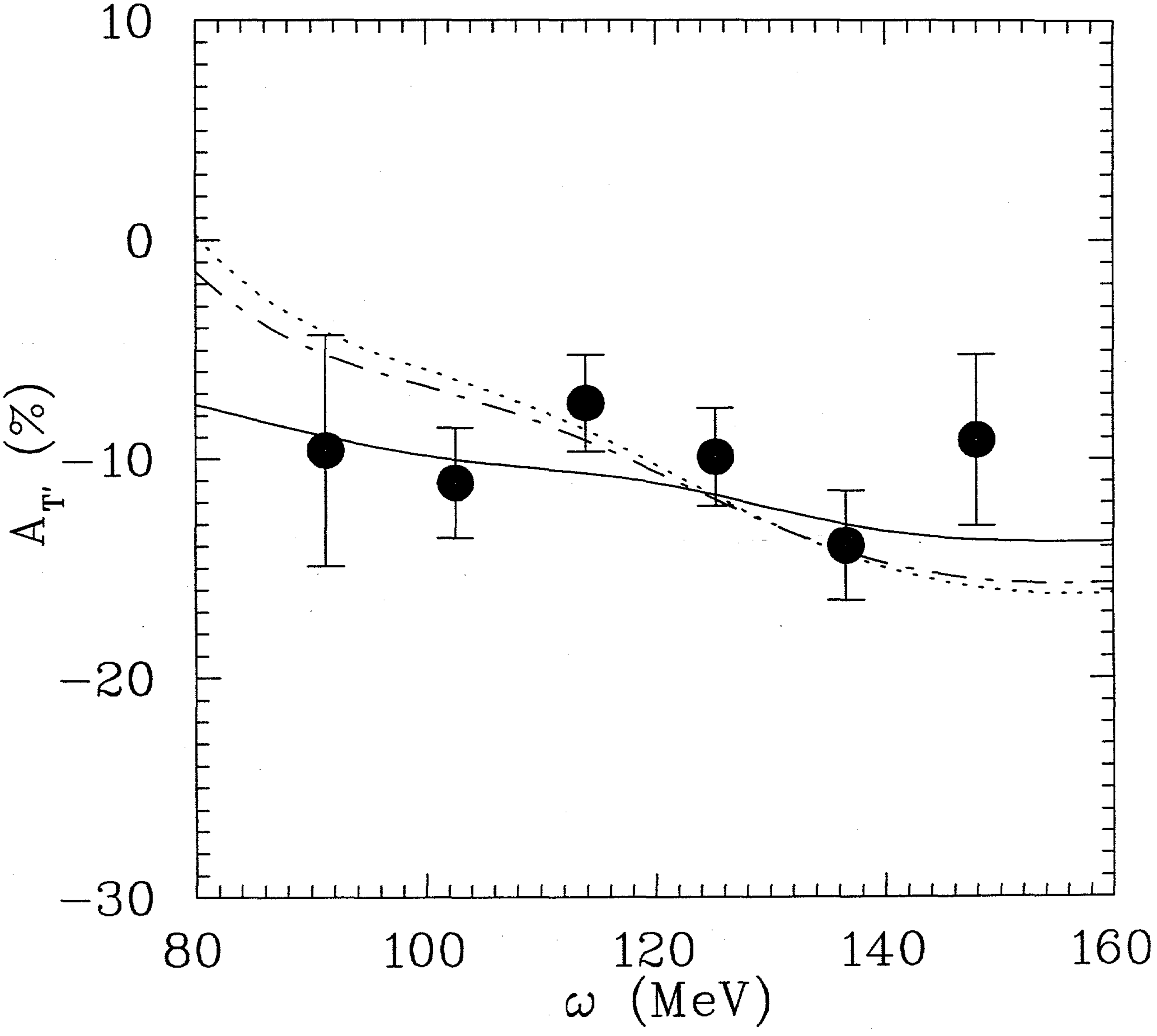

Fig. 1

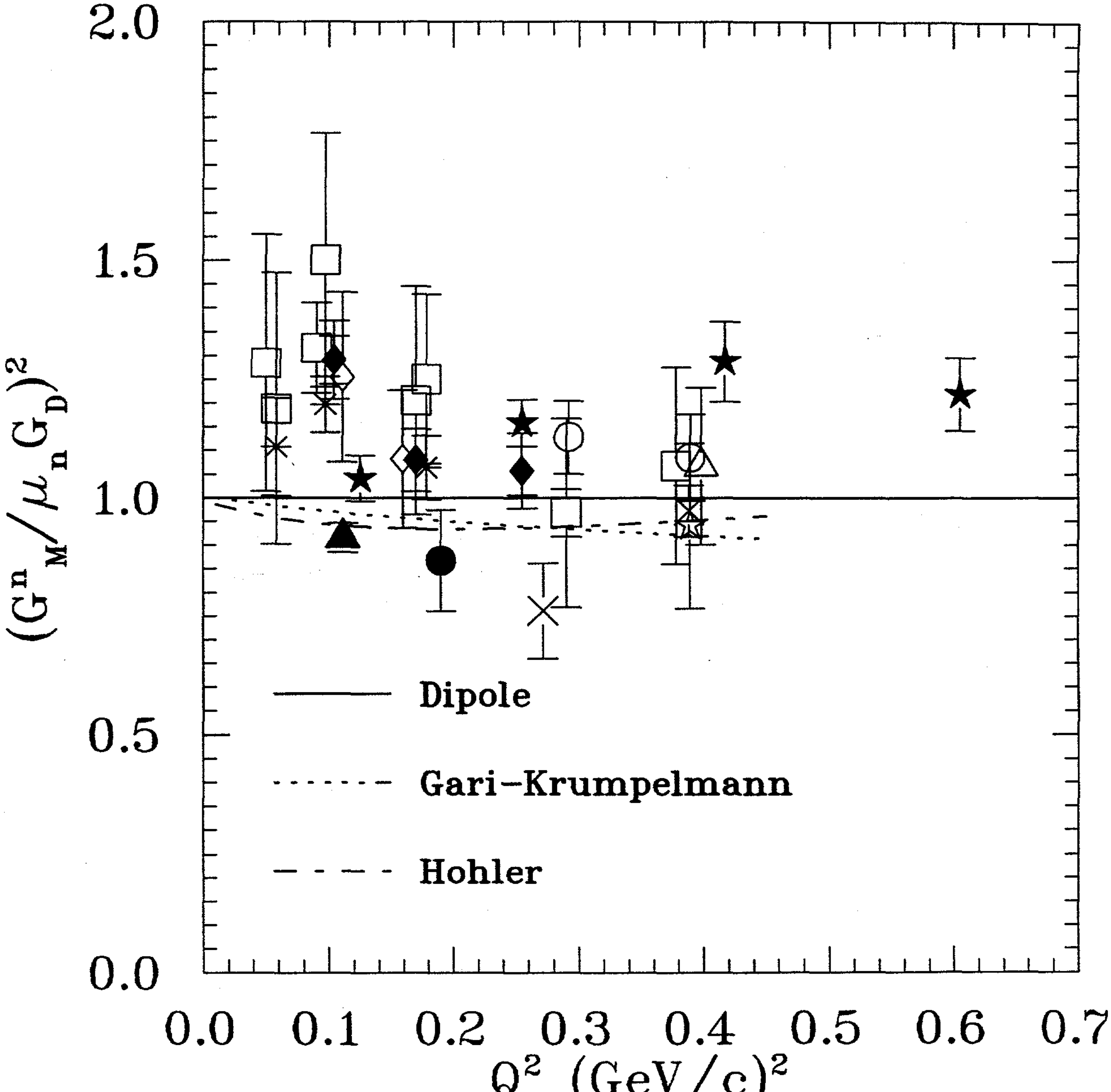
2.0
1.5
1.0
0.5
0.0
$(G^n_M/\mu_n G_D)^2$
0.0
0.1
0.2
0.3
0.4
0.5
0.6
0.7
Q^2 (GeV/c)^2
Dipole
Gari–Krumpelmann
Hohler

Fig. 2

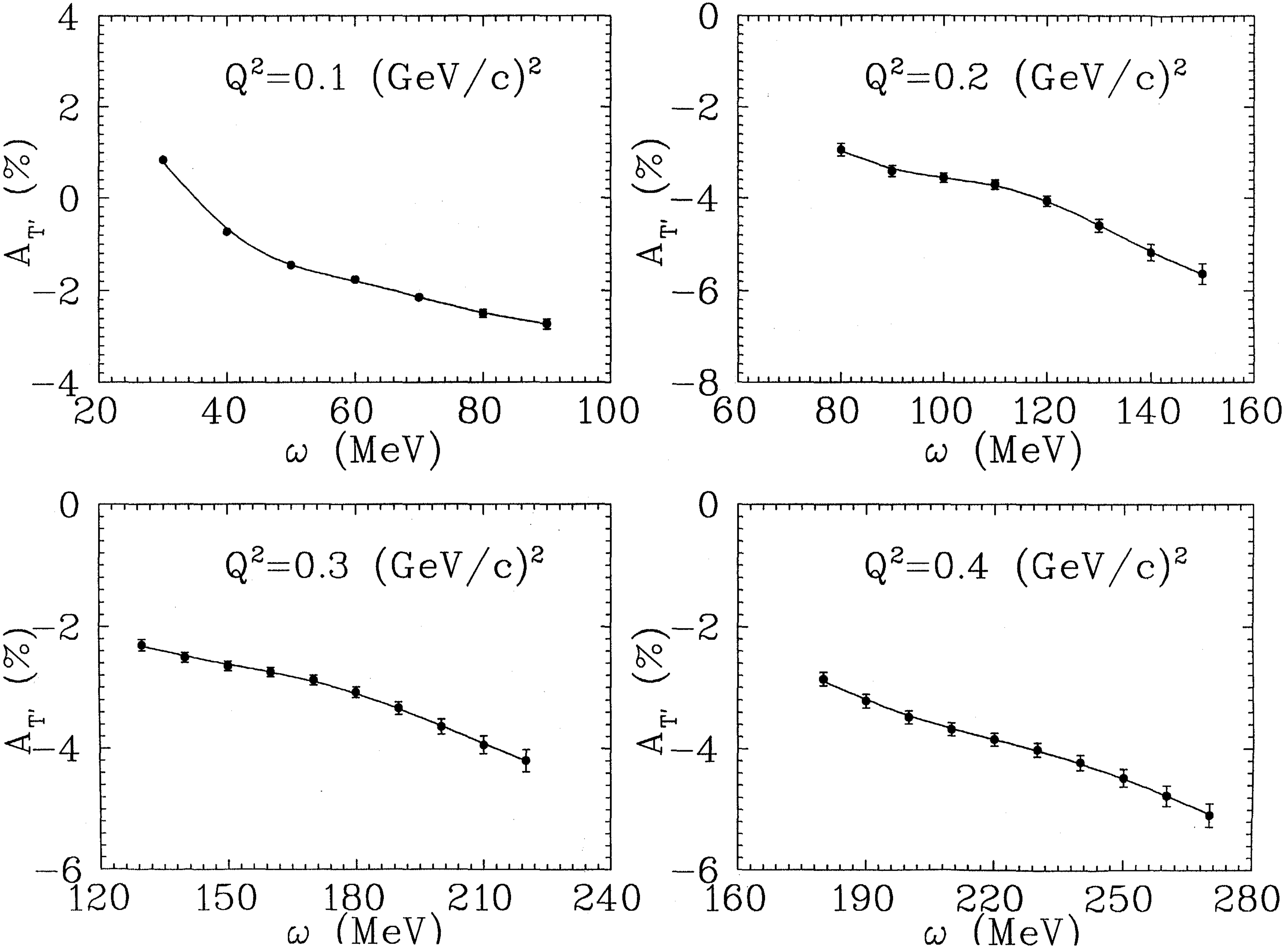
Q^2=0.1 (GeV/c)^2
Q^2=0.2 (GeV/c)^2
Q^2=0.3 (GeV/c)^2
Q^2=0.4 (GeV/c)^2
$A_{T'}$ (%)
ω (MeV)
4
2
0
−2
−4
20
40
60
80
100
−8
−6
60
80
100
120
140
160
120
150
180
210
240
160
190
220
250
280

Fig. 3

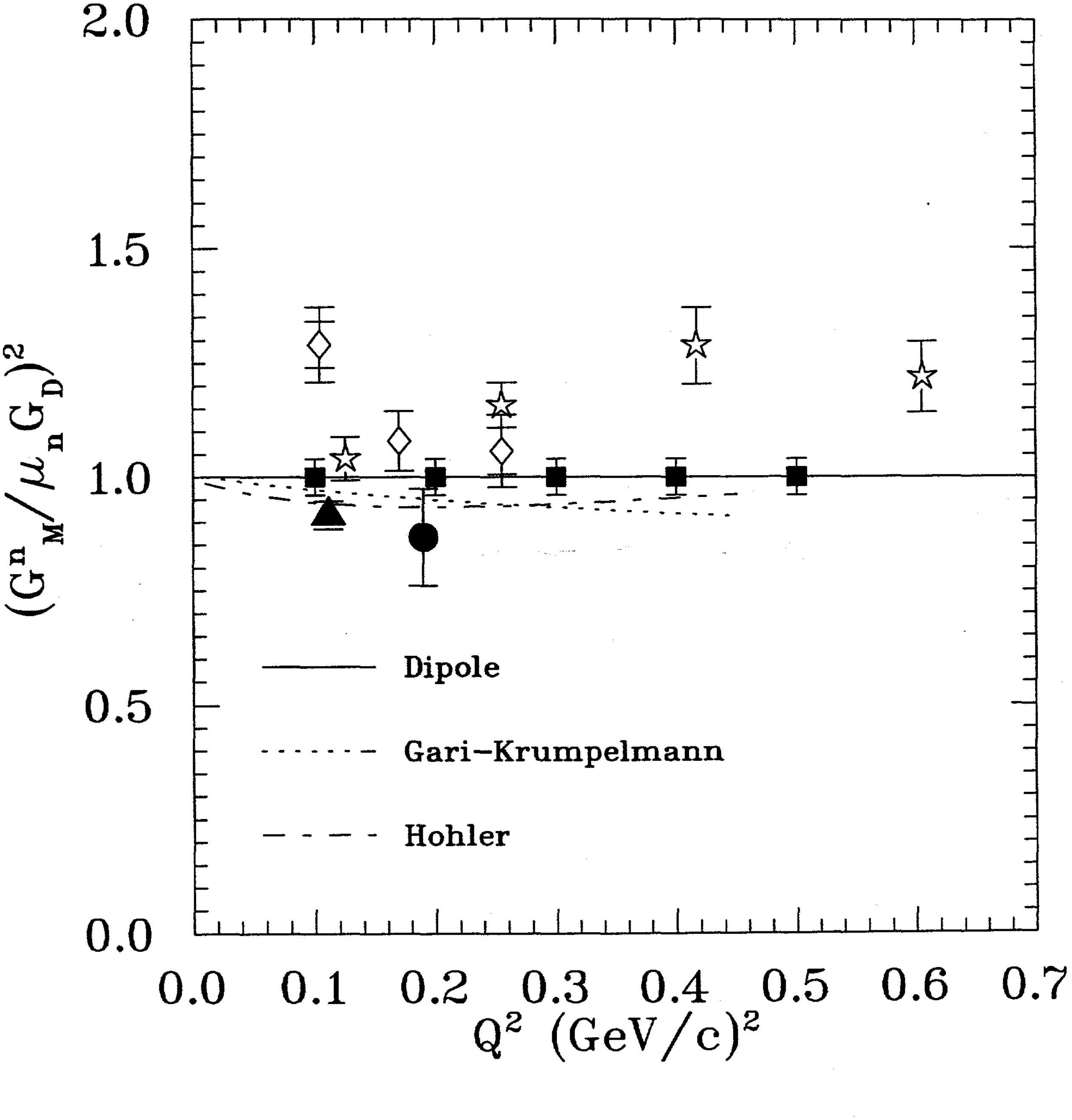
2.0
1.5
1.0
0.5
0.0
0.0
0.1
0.2
0.3
0.4
0.5
0.6
0.7
$(G^n_M/\mu_n G_D)^2$
Q^2 (GeV/c)^2
Dipole
Gari–Krumpelmann
Hohler

Fig. 4